LANGMUIR

pubs.acs.org/Langmuir Article

Universal Method Based on Layer-by-Layer Assembly for Aptamer-Based Sensors for Small-Molecule Detection

Ksenia A. Rukhlyada,[#] Victoria V. Matytcina,[#] Anna A. Baldina, Olga Volkova, Dmitry A. Kozodaev, Nadezhda V. Barakova, Olga Yu. Orlova, Evgeny Smirnov, and Ekaterina V. Skorb*

Cite This: *Langmuir* 2023, 39, 10820–10827 Read Online

ACCESS | Metrics & More | Article Recommendations | Supporting Information

ABSTRACT: Development of a fast and accurate pesticide analysis system is a challenging task, as a large amount of commonly used pesticide has negative effects on humans' health. Detection of pesticide residues is crucial for food safety management and environmental protection. Aptamers—short single-stranded oligonucleotides (RNA or DNA) selected by aptamer selection method SELEX—can selectively bind to their target pesticide molecules with high affinity. Thus, in the present study, we developed an electrochemical biosensor based on aptamers to detect the commonly used pesticide, glyphosate. Carbon fibers were used as the platform to assemble polyelectrolyte layers with the incorporated aptamers selectively binding with glyphosate molecules for electrochemical detection. The best limit of detection of 0.3 μM was achieved at open-circuit potential measurements, which is comparable to the current need in detection of glyphosate. The developed method can be implemented into existing systems for the determination of pesticides on farms to control residual concentrations of glyphosate in soil and water.

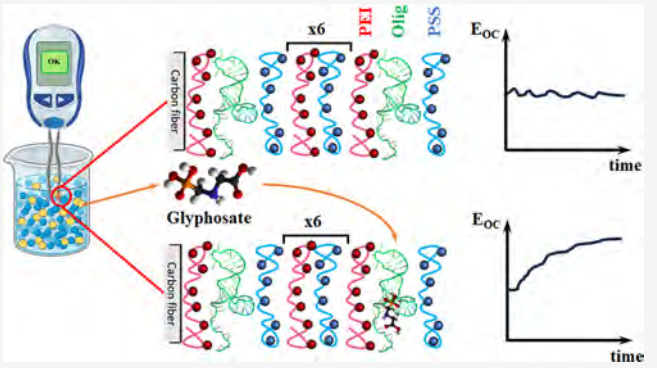

INTRODUCTION

The systematic use of chemicals to protect crops from harmful plants, parasites, and bacteria began in the second half of the nineteenth century. Those chemical or biological compounds were called pesticides and were used to control plant pests and weeds as well as to increase the gross harvest of plant raw materials.[1,2] Over the past 40 years, the use of pesticides in agriculture has increased significantly leading to inability to grow agricultural products without them. However, today the pollution of water, soil, atmosphere, and even food by pesticides has become a global challenge.

Systemic herbicides are one of the most effective weed killers that absorb and transport through the plant's vascular system, killing the entire plant.[1] Recently, several methods have been developed for the effective decomposition of pesticides such as nanomaterials and nanocomposites based on TiO_2 and Fe^0;[2] however, their metabolic products may turn out to become even more toxic[3] and resistant than the original compounds.[4]

Pesticides may enter the human body both directly and indirectly. The direct way is consuming poisoned water or breathing aerosols from farms, whereas the indirect way consists of consuming animal products that have eaten food treated with pesticides. Consumed pesticides may cause various forms of cancer,[5] mental disorders,[6] and poisoning.[7] Studies linking the use of pesticides and cancer have shown a relationship between exposure to pesticides and the development of certain types of cancer, especially for children.[8]

Glyphosate (Gly) is an *N*-phosphonomethyl derivative of the amino acid glycine. It is a non-selective systemic herbicide used to control weeds, especially perennial weeds. In terms of production, Gly ranks the first among herbicides in the world. Additionally, these molecules became a part of the most chemical plant-protection products used in crop production despite adsorption in the soil and slight penetration into groundwater.[9] Recently, the concern has increased worldwide about the potential direct and indirect health effects of a large-scale usage of Gly. In 2015, the World Health Organization classified Gly as carcinogenic compounds to humans.[10] When studying transgenic-resistant crops, the use of Gly created a "pesticide paradox". The pesticide paradox states that the use of pesticides to a harmful organism may eventually lead to an increase in the number of harmful organisms. Thus, Gly is the most widely used herbicide and one of the most defined.[11]

Received: March 27, 2023
Revised: July 11, 2023
Published: July 25, 2023

https://doi.org/10.1021/acs.langmuir.3c00822
Langmuir 2023, 39, 10820−10827

To date, the residual content of pesticides in raw materials and water samples is determined primarily by conventional methods such as gas chromatography (GC)[12] or liquid chromatography (LC),[13] capillary electrophoresis with indirect UV detection,[14] and mass spectrometry.[15] These analytical methods require high-qualifying labor, time-consuming sample preparation procedures, and complex instrument installations and take a lot of time, which makes their use quite complicated.[16] To address these challenges, biosensors have been developed to detect pesticide residues.

Biosensors are analytical devices made of two important functional components: the target recognition element (responsive for high accuracy) and the transducer element (responsive for low signal-to-noise ratios and fast sampling frequency). According to their transducer element, biosensors can be divided into optical biosensors, electrochemical biosensors,[17] enzymatic biosensors, tissue biosensors, immunosensors, DNA biosensors, thermal biosensors, and piezoelectric biosensors.[18] These biosensors are more convenient and easy to use than traditional methods, as well as applicable to field tests with fast, specific, and highly sensitive detection.[19] Moreover, biosensor systems are of considerable interest due to their ability to continuously provide information in real time.

Aptamer-based biosensors were considered as excellent candidates for detection of pesticides in comparison with commonly used antibodies or enzymes because they possess better stability, lower molecular weight, easer of modification, and lower cost.[20] Thus, common DNA biosensors were developed based on the affinity of a single-stranded nucleic acid molecule to its complementary DNA chain in a sample. The interaction occurs due to the formation of stable hydrogen bonds between two strands of nucleic acids.[21] Similarly, short single DNA called oligomers or aptamers can interact strongly with other molecules such as pesticide, antibodies, metal ions (e.g., K^+, Hg^{2+}, and Pb^{2+}), small organic molecules (e.g., amino acids, ATP, antibiotics, and vitamins), organic dyes, peptides, and proteins (e.g., thrombin, growth factors, and HIV-associated peptides).[22] Recently, several aptamer-based biosensors for detecting pesticides have been developed.[23] For example, electrochemical aptasensors have demonstrated great potential for detecting pesticides due to their fast response, high sensitivity, specificity, low cost, and possibility of multiplex analysis.[24] Due to these advantages, the use of aptamers is a promising alternative[25] to the traditional pesticide detection methods.

Biosensors require a solid support. In this regard, conductive material such as carbon fiber is an inexpensive commercially available and promising material for creating flexible devices. In addition, carbon materials possess good biocompatibility, which is necessary for the manufacture of biosensors.[26] In this case, the sensor layer can be made using the method of layering polyelectrolytes on the substrate.

Layer-by-layer (LbL) assembly is one of the ways to produce thin films based on alternating adsorption of complementary multivalent compounds on a substrate through electrostatic interactions, hydrogen bonds, or other secondary interactions. The LbL technique allows controlling the composition of the film and creating complex compositions of coatings that will maintain the activity of sensitive molecules at room temperature.[27] The assembly of LbL films with polyelectrolytes uses the ability of polyelectrolytes to self-organize into supramolecular structures. Such supramolecular structures can be used as a highly selective matrix to ensure the effective interaction of an oligonucleotide with specific molecules.[28]

Therefore, in this work, we introduce a novel biosensor for pesticides. It is based on oligomers incorporated into a soft polymer matrix consisting of PEI-PSS-alternating layers and containing oligos for selective detection of pesticides. The approach was first investigated by QCM and then integrated into electrochemical systems.

EXPERIMENTAL SECTION

Chemicals and Materials. Potassium hexacyanoferrate(III) $K_3[Fe(CN)_6]$, poly(sodium 4-styrenesulfonate) (PSS, M_w 500 kDa), polyethyleneimine (PEI, M_w 70 kDa, 50 wt % water solution), and potassium chloride (KCl) were purchased from Sigma-Aldrich. Hydrogen peroxide and phosphate-buffered saline tablets for preparation of PBS (pH 7.4) were purchased from Biolot (Russia). Gly, aminomethylphosphonic acid (AMPA), and *N*-(phosphonomethyl)iminodiacetic acid (PMIDA) were purchased from Aldrich (USA). All chemicals were used without further purification.

The oligonucleotide was purchased from DNA Synthesis company (Moscow, Russia) and is listed as follows: AAGCTTGCTTTA-TAGCCTGCAGCGATTCTTGATCGG. The Gly (*N*-(phosphonomethyl)glycine) was purchased from Sigma-Aldrich (USA).

Carbon fibers (CFs) with 450 g/m^2 of area density were purchased from M-Carbo (Minsk, Belarus). Silver conductive glue was purchased from Kontakt (Keller). The CFs were conditioned in 3 M KCl.

All solutions were prepared with deionized water (18.2 MΩ.cm, 25 °C, Millipore Milli-Q).

Screen-printed carbon electrodes were purchased from ItalSens (PalmSens, Italy).

Oligonucleotide Preparation. The solution of aptamers with concentrations of 1, 2.5, and 5 μM was prepared by diluting lyophilized oligonucleotides in nuclease-free water.

Self-Assembly of Polyelectrolyte Layers. The last layer of the matrix was represented by Gly molecules (Scheme 1).

Scheme 1. Schematic Representation of the DNA-Based Electrochemical Sensor for Gly Detection[a]

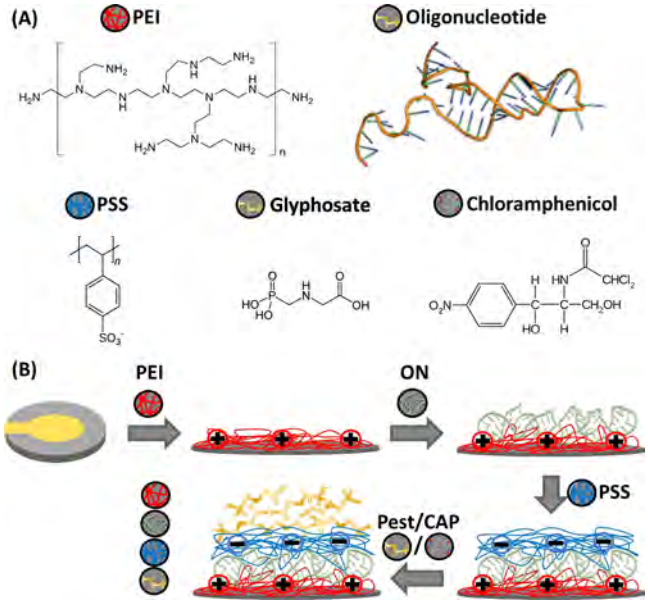

[a](A) Structures of used molecules. (B) The gold electrode was subsequently modified with polyelectrolyte layers (PEI-PSS) and oligonucleotide (ON), pesticide (Pest), chloramphenicol (CAP).

https://doi.org/10.1021/acs.langmuir.3c00822
Langmuir 2023, 39, 10820−10827

The general scheme of modification of the electrode surface by a polymer matrix consisting of layers of charged polyelectrolytes is shown in Scheme 1.

The first layer of polyelectrolyte assembly was formed with cationic polyelectrolyte PEI because of its advantage in uniform distribution on the semiconductor surface with micron-sized thickness, as shown previously.[29]

Oligonucleotide molecules were charged negatively due to a phosphate group at the 3′-terminal,[30] thus favoring the formation of polyelectrolyte complexes with PEI linked by electrostatic interactions. The next layer was formed by addition of negatively charged PSS to compensate for retained positive charge and increase the entanglement of chains in polyelectrolyte layers.[31]

QCM Measurements. The electrochemical quartz crystal microbalance method was used with eQCM 10M (Gamry, USA). The 5 MHz coated QCM crystal (Shenzhen Renlux Crystal Co., Ltd., China) was fixed into the detection cell. The measurements were performed in a flow cell connected to the potentiostat (Gamry Instruments, USA) using flow cells. All solutions have flown into the modules at a flow rate of 0.5 mL/min by using a peristaltic pump BT100LC (Baoding Chuangrui Precision Pump Co., Ltd., China) at 7.1 RPM.

Electrodes for eQCM were cleaned with a hot mixture of piranha solution (a 1:3 mixture of 30% (v/v) H_2O_2/conc. H_2SO_4) for 5 min and then washed in deionized water several times. **Caution:** The piranha solution represents a potential hazard; therefore, it has to be handled with special care.

Changing the fundamental frequency of the QCM resonance depends on the thickness of the quartz plate, d, besides the physical constants of the quartz crystal, in accordance with the following Sauerbrey equation:

$$\Delta m = \frac{A\sqrt{\mu\rho}}{2f_0^2}\Delta f \quad (1)$$

where f_0 is the resonant frequency of the fundamental mode (Hz), Δf is the normalized frequency change (Hz), Δm is the mass change (g), A is the active quartz crystal area (area between electrodes, cm^2), μ is the density of quartz (= 2.648 g/cm^3), and ρ is the shear modulus of quartz for the AT-cut crystal (= 2.947 × 10^{11} $g{\cdot}cm^{-1}{\cdot}s^{-2}$).

The Sauerbrey equation is strictly valid only for an infinite resonator disk. In real devices, the quartz size is confined and the electrodes occupy a part of the quartz surface. In this configuration, the magnitude of the oscillations is unevenly distributed; therefore, the oscillations will be limited to the area of the electrodes and will quickly disappear outside the electrodes.[32] Because of these imperfect effects, the Sauerbrey approximation must be experimentally confirmed, particularly when the coating film is not rigid enough and is distributed unevenly, for example, in the case of polymer or molecular layers.[33]

SPCE Surface Modification. The 5 μL PEI solution (2 mg/mL in deionized water) was spotted onto the electrode surface, dried, and rinsed three times with water to remove excess PEI. Then, 5 μL of oligonucleotide solution (2,5 μM in water) was added, dried, and washed three times with DI water. Drying the surface is necessary to compact layers, increase layer-to-layer interactions, and prevent layer washing out.

In the next step, 5 μL of PSS solution (2 mg/mL in deionized water) was added, dried, and washed similarly to PEI solution. Then, 5 μL of Gly solution (2,5 μM in deionized water) was added, dried, and washed with water.

CF Surface Modification. CFs were cut into 80 mm-length pieces and then covered with parafilm, leaving 15 mm uncovered at both ends. Following this step, one of the ends was coated with silver conductive glue and left to dry in air for 30 min. After that, the end coated with silver was immersed into 1 M HCl and rinsed with deionized water to make AgCl coating on the CF surface (Scheme 2).

The working area of the electrode was modified using the LbL assembly according to the procedure adapted from ref 34. The LbL deposition of the polyelectrolyte film was carried out to the CF over a layer of silver sub-layer. The film consisted of PEI, oligonucleotide, and PSS layers. Thus, the electrode was plunged sequentially for 30 s into

Scheme 2. Carbon Fiber Modification Process.[a]

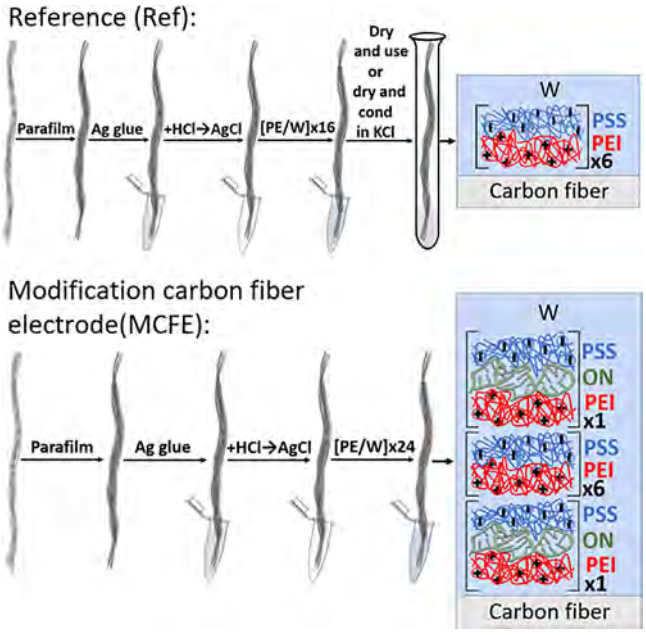

[a]The architecture of the reference electrode was $(PEI/PSS)_8$. The modified carbon fiber electrode (MCFE) has a composition of (PEI/oligonucleotide/PSS)$(PEI/PSS)_6$(PEI/oligonucleotide/PSS). PE/W describing polyelectrolyte deposition and washing with DI water steps.

PEI solution at first and then in oligonucleotide solution, and finally into PSS solution. The procedure was repeated eight times leading to the following layer configuration (PEI/oligonucleotide/PSS)$(PEI/PSS)_6$(PEI/oligonucleotide/PSS). For the reference electrode, a similar procedure was applied, except for addition of oligonucleotide, leading to $(PEI/PSS)_8$ configuration without oligonucleotide. All the described modifications are present in Scheme 2.

Drying of polyelectrolyte layers was carried out by suspending the electrode vertically for 40−90 min at room temperature. After modification, the electrodes were conditioned in a 3 M KCl solution.

Electrochemical Measurements. When the analyzed substances are in the environment of the substance, a target-induced signal is generated and recorded as the corresponding electrochemical signal.[35] The prepared electrodes were tested in the solution containing 5.0 mM $K_3[Fe(CN)_6]$.

Cyclic voltammetry (CV) was recorded with a PalmSens4 potentiostat (PalmSens, The Netherlands). The potential was cycled between −0.8 and +0.6 V (vs Ag/AgCl) at a scan rate of 50.0 mV s^{-1}.

Potentiometric Measurements for CF Electrodes. After LbL modification, the electrodes and CVs from the prepared electrodes were measured within a potential range from −1.3 to +1.3 V in a 1 M KCl solution with different concentrations of the pesticide (from 0.625 to 5 μM). The peak current served as an analytical signal.

Another route for detecting the presence of redox molecules close to the electrode surface is open-circuit potential (OCP or E_{OC}). In the presence of redox species close to the electrode surface, the electrode potential will equilibrate with one of redox species;[36,37] there is no current flow in the system. Due to the specific interaction of pesticide and oligonucleotide, measuring OCP provides information about the concentration of pesticide in the close vicinity of the electrode.

Potential measurements between the reference and working electrodes were carried out using a Potentiostat/Galvanostat SP50 (Electrochemical Instruments, Russia) in a standard two-electrode cell at room temperature (23 °C)[38] in a solution of 1 M KCl with Gly.

Atomic Force Microscopy Measurements. AFM measurements were carried out on a SmartSPM 1000 (AIST-NT, Russia) scanning

https://doi.org/10.1021/acs.langmuir.3c00822
Langmuir 2023, 39, 10820−10827

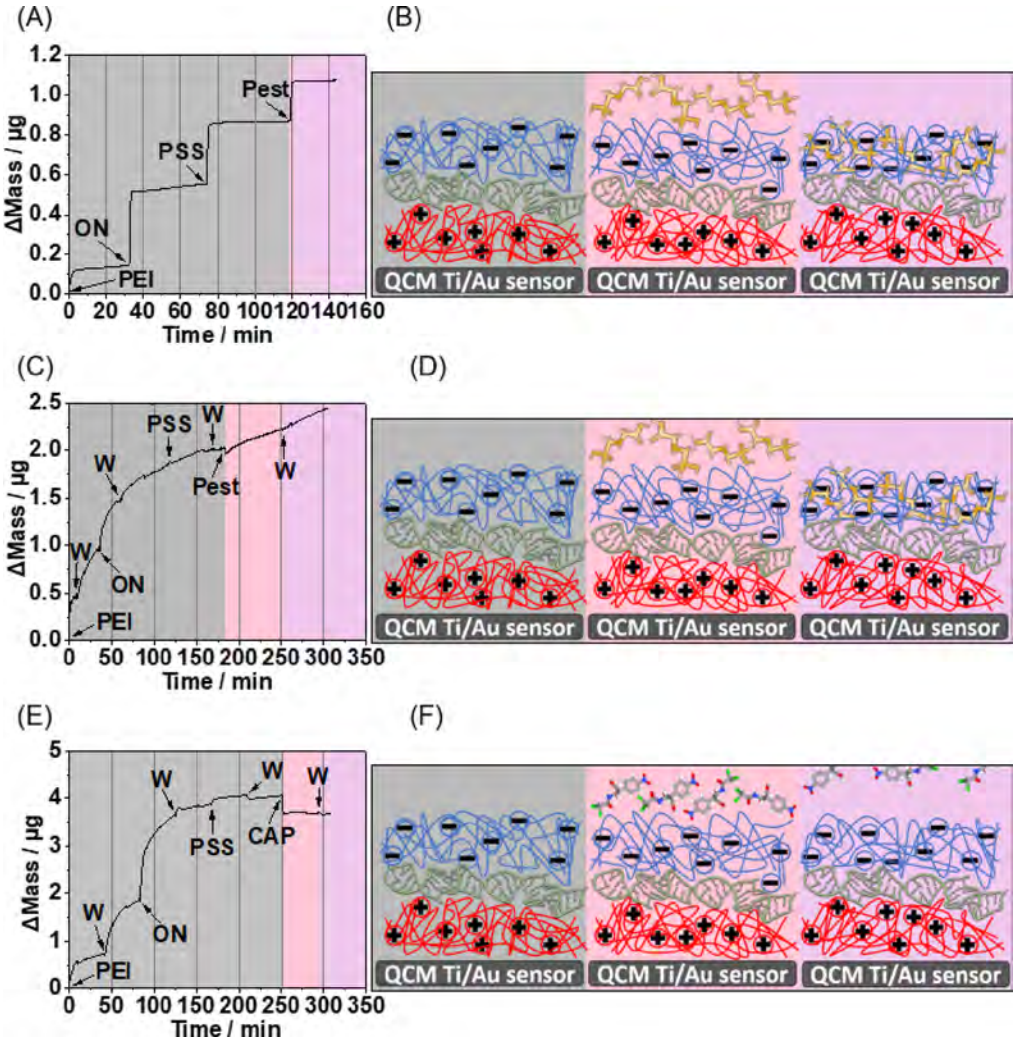

Figure 1. Formation of aptamer−pesticide and aptamer−antibiotic complexes in the polymer matrix by the QCM method. (A) Mass change during the formation of successive layers consisting of PEI/oligonucleotide/PSS/pesticide and (B) process schematic. (C) Mass change during the formation of successive layers consisting of PEI/wash/oligonucleotide/wash/PSS/wash/pesticide/wash and (D) process schematic. (E) Mass change during the formation of successive layers consisting of PEI/wash/oligonucleotide/wash/PSS/wash/CAP/wash and (F) process schematic representation.

Table 1. Average Mass-Shift Values from the QCM Measurements

QCM measurement	compound	mass (μg)	mass change (μg)
(A) PEI/ON/PSS/pest	PEI	0.143	0.143
	PEI/ON	0.551	0.408
	PEI/ON/PSS	0.869	0.318
	PEI/ON/PSS/pest	1.074	0.205
(B) PEI/W/ON/W/PSS/W/pest/W	PEI/W	0.903	0.903
	PEI/W/ON/W	1.811	0.908
	PEI/W/ON/W/PSS/W	1.992	0.181
	PEI/W/ON/W/PSS/W/pest/W	2.260	0.268
(C) PEI/W/ON/W/PSS/W/CAP/W	PEI/W	1.885	1.885
	PEI/W/ON/W	3.862	1.978
	PEI/W/ON/W/PSS/W	4.051	0.189
	PEI/W/ON/W/PSS/W/CAP/W	3.651	−0.401

probe microscope in tapping mode using semi-contact Si cantilever probes (typical curvature radius 6−8 nm).

RESULTS AND DISCUSSION

Quartz Crystal Microbalance (QCM) as a Tool to Choose the Polymer-Matrix Layer Structure for the Biosensor. The simplest combination of polycation and polyanion layers with an oligonucleotide located between them, such as PEI/Oligonucleotide/PSS, was investigated (Figure 1).

To show specific and non-specific interactions of the oligonucleotide and Gly in the matrix of polyelectrolytes, the

https://doi.org/10.1021/acs.langmuir.3c00822
Langmuir 2023, 39, 10820−10827

adsorption of polyelectrolytes, oligonucleotide, and Gly on electrodes was conducted using the QCM method.

The oligonucleotide layer was completely covered by a negatively charged polymer. In this case, the interaction of the aptamer with Gly molecules occurs on the surface of the matrix. To monitor non-specific interactions of the oligonucleotide, the antibiotic chloramphenicol was used instead of Gly. The antibiotic contains similar pesticide motifs such as −NH−C═O− but with different other substitutes. The mass changes during deposition on QCM chips are shown in Figure 1 and summarized in Table 1.The addition of each molecule such as PEI, oligonucleotide, PSS, or Gly led to a subsequent mass increase (Figure 1A,B, Table 1A) that can be explained as deposition of the layer to the electrode.

When the formed structure—PEI/oligonucleotide/PSS/Gly—was washed with deionized water, ions were washed out of the layers, which led to compensation of charges inside the layers due to the electrostatic attraction of macromolecules and, consequently, to the compaction of the nanolayers.

In turn, the compaction of nanolayers caused a decrease in the frequency of microbalances reflecting an increase in mass (Figure 1C,D, Table 1B).

In the case when antibiotic chloramphenicol (CAP) was used instead of Gly (Figure 1E,F, Table 1C), the addition of chloramphenicol after the PSS layer led to rapid leaching of the antibiotic from the surface deeper into the PSS layer. These results indicate that the interaction between aptamer and Gly is specific whereas with CAP it is non-specific.

Electrochemical Determination of Gly. Proof of Concept with Modified Screen-Printed Carbon Electrodes (SPCE). Cyclic voltammograms were recorded on the modified SPC electrode with different Gly concentrations in solution to confirm the accessibility of the electrode surface for electrochemical reactions. A solution of 5 mM redox couple $[Fe(CN)_6]^{3-/4-}$ were chosen. Figure 2 demonstrates changes in CVs during addition of polyelectrolyte layers as well as with increasing of the Gly concentration.

Thus, addition of PEI to the SPCE surface led to an increase in current and to a slight shift of the redox potential (Figure 2B, Table 2).

The latter can be explained, most likely, because of an additional Coulombic interaction between positively charged PEI and negatively charged redox couple. The following addition of oligonucleotide (ON) to the PEI layer resulted in current decrease, as part of the electrode became blocked by non-conductive or less conductive DNA whereas the redox potential did not shift much. The final layer of the negatively charged polymer led to a significant decrease in current and an increase in anodic-to-cathodic peak separation (up to ca. 500 mV). It can be understood as Coulombic repulsion between the negative charge of both polymers and the redox couple increase, and charged bi-layer PEI-PSS at the electrode surface was formed (Table 2). Increasing the pesticide concentration used in experiments after SPC-electrode modification primarily led to higher peak current values without a significant shift of the potential (except only very high pesticide concentrations), as depicted in Figure 2C and Table 2.

Additionally, based on data presented in Figure 2C, the limit of detection (LOD) was calculated as 0.56 μM.

LbL-Modified CF Electrodes. CF was chosen to reduce the cost of the electrode and, thus, lower the overall cost of the proposed method. The desired electroanalytical characteristics were achieved using miniature electrodes modified with

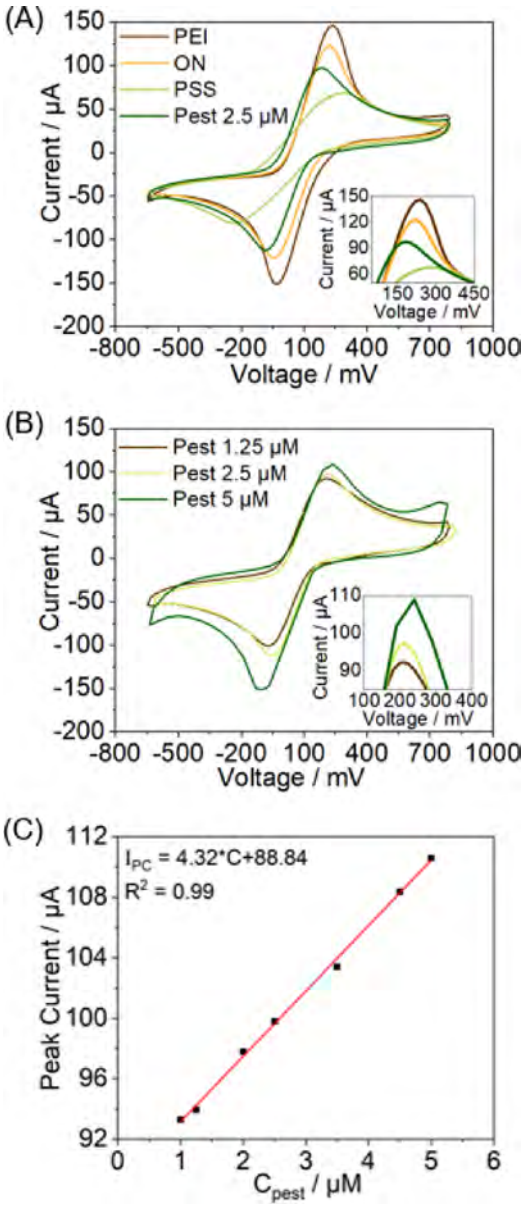

Figure 2. Electrochemical characterization of SPC electrodes at various film composition and pesticide concentrations. Scan rate was 50 mV s^{-1}. Recorded CVs (A) at different electrode layer compositions and (B) at selected glyphosate concentrations. (c) Evolution of peak currents at different glyphosate concentrations.

polyelectrolytes by analogy with ion-selective electrodes in ref 39. The CF surface was modified according to the procedure described in detail in the Chemicals and Materials section (MCFE). The main difference between the MCFE and the reference electrode is the top and bottom layers containing the oligonucleotide in the case of the MFCE. Such modifications led to nanostructured electrodes with a polyelectrolyte matrix and an oligonucleotide included in it, which can specifically absorb the pesticide, as shown vide supra. To characterize the surface of the functionalized CF electrodes, AFM was applied revealing the characteristic surface coverage of the CF electrode with PEI-PSS bilayers. The roughness of the surface increased by 10% (Section 3 in the Supporting Information).

First, modified MCF electrodes with addition of 2.5 μM of oligonucleotide were characterized with cyclic voltammetry in solution containing pesticide with concentrations in the range of

https://doi.org/10.1021/acs.langmuir.3c00822
Langmuir 2023, 39, 10820−10827

Table 2. Analysis (Peak Currents and Potentials, $E_{1/2}$, and Peak to Peak Separation, ΔE) of the Obtained Electrochemical Data on the SPC-Electrode Covered with Polyelectrolyte Layers and at Different Pesticide Concentrations

	layer added	E_{ac} (mV)	I_{ac} (μA)	E_{pc} (mV)	I_{pc} (μA)	$E_{1/2}$ (mV)	ΔE (mV)
Figure 2A	PEI	240	146	−26	−152	107	266
	ON	221	123	−47	−122	87	268
	PSS	281	68	−227	−82	27	508
	pest 2.5 μM	181	97	−87	−113	47	268
Figure 2B	C_{pest} (μM)						
	1.25	201	92	−67	−102	67	268
	2.5	210	98	−58	−113	76	268
	5	340	109	−103	−151	118.5	443

0.5 to 4.5 μM and 1 M KCl as the supporting electrolyte (Figure 3A). It demonstrates cathodic and anodic processes with quite

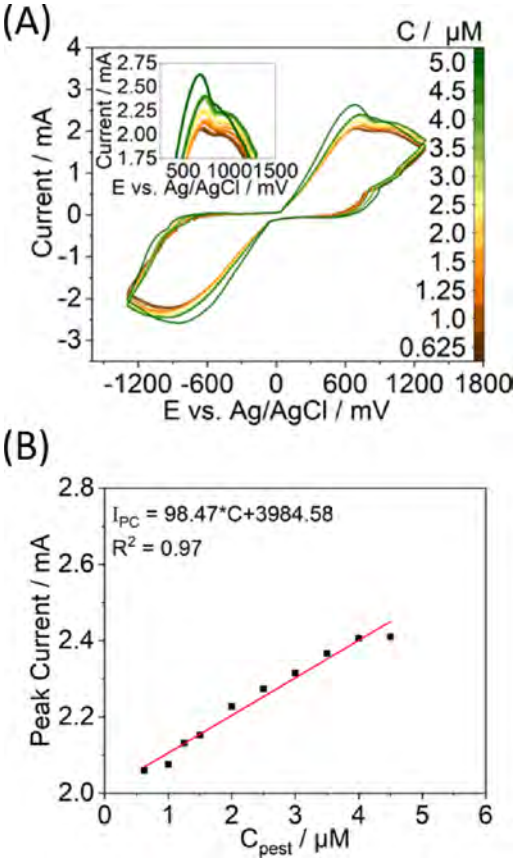

Figure 3. Electrochemical characterization of MCF electrodes at different pesticide concentrations. (A) CVs at different concentrations of Gly in 1 M KCl solution. The scan rate was 50 mV s^{-1}. (B) Peak current dependence on Gly concentrations in the solution and linear approximation of experimental data.

large separation (more than 1000 mV). Nevertheless, the peak current changes along with the concentration of pesticide in the solution; moreover, it shows linear dependence of the current on the Gly concentration (Figure 3B).

Second, the MCF electrodes were characterized via OCP (E_{OC}). As the pesticide molecule penetrates a soft matrix of polyelectrolytes at the electrode surface and forms a complex with oligonucleotide, it changes the charge density distribution close to the electrode. The latter affects E_{OC} that can be used to probe the presence of pesticide and measure its concentration. In this scenario, a reference electrode without the oligonucleotide is necessary for accurate measurement of OCP.

Initially, OCP was measured for the modified electrode at conditioning in 3 M KCl (OCP_1) and then in the solution containing pesticide and 1 M KCl (OCP_2), and the resulting change in OCP was calculated as the following:

$$\Delta E_{OC} = OCP_2 - OCP_1 \quad (2)$$

Measured ΔE_{OC} for varying concentrations of pesticide and three different concentrations of oligonucleotide in the biosensor are present in Figure 4. Overall, considering the

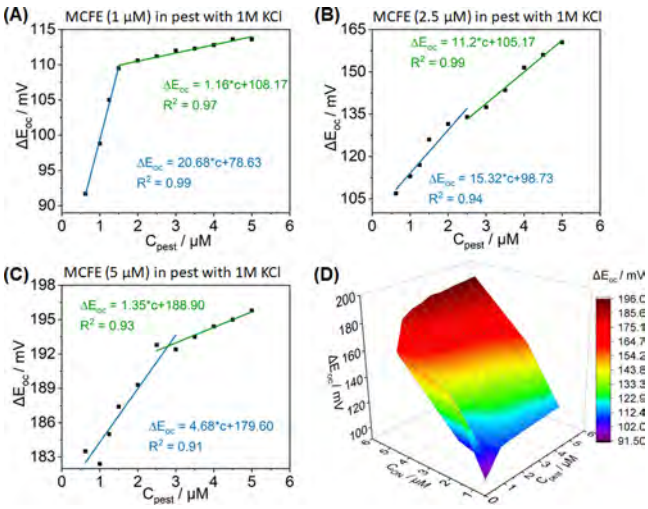

Figure 4. Open-circuit potential change for MCF electrodes in solutions with different concentrations of glyphosate, ranging from 0.5 to 4.5 μM. The concentration of oligonucleotide in the polyelectrolyte matrix was (A) 1 μM, (B) 2.5 μM, and (C) 5 μM. (D) 3D plot of the (A−C) dependencies.

concentrations of oligonucleotide in the sensor, ΔE_{OC} increased with the presence of pesticide molecules (Figure 4a−c). The latter indicates accumulation of pesticide molecules in the matrix because of specific interactions with the oligonucleotide. Additionally, the obtained data were replotted as a 3D graph for better visualization.

Interestingly, the ΔE_{OC} dependence on pesticide concentration consisting of two parts split at the vicinity of the concentration matching with the oligonucleotide's concentration. Higher sensitivity or higher slope was observed if the pesticide concentration is lower than that of the oligonucleotide, whereas the sensitivity lowers if the pesticide concentration overcomes that of the oligonucleotide. Speculatively, the latter can be understood as follows: excess of oligonucleotide leads to stronger binding, fast accumulation, and negligible pesticide desorption, which stops around the 1:1 composition; after that limit, pesticide molecules start to compete for binding, which leads to dynamic equilibrium and drops in sensitivity.

Molecules structurally similar to Gly molecules such as AMPA and PMIDA were also examined with E_{OC} measurements; however, they demonstrated minor influence on the E_{OC} (Section 4 in the Supporting Information).

https://doi.org/10.1021/acs.langmuir.3c00822
Langmuir 2023, 39, 10820−10827

Finally, the LOD was estimated based on linear equations for the lower part of pesticide concentration. The LODs for the first linear region were calculated to be 0.30, 0.51, and 0.67 μM for the 1, 2.5, and 5 μM oligonucleotide concentrations, respectively.

CONCLUSIONS

To conclude, we demonstrated a novel electrochemical biosensor based on oligonucleotides incorporated into the soft polymer matrix with strong capacity to detect selectively micromolar concentrations of pesticide such as Gly. Using an aptamer possessing a high affinity and specificity to the target molecule as an anchor allows achieving high sensitivity and selectivity for the biosensor. The specific interactions between oligonucleotide and pesticide led to accumulation and concentration of pesticide molecules in the vicinity of the electrode surface, enabling easy and uncomplicated electrochemical detection such as CV and OCP measurements both qualitatively and quantitatively. The best achieved LOD in OCP measurements was 0.3 μM, which is in line with current needs to control over this pesticide. At the same time, the high selectivity was confirmed in the detection of chloramphenicol by the QCM method that demonstrated non-specific adsorption. The manufacturing process for CF electrodes based on LbL self-assembly can be completely automated, opening the door to an entirely robotized analytical system. Moreover, the structure and composition of oligonucleotides can be tuned to fit any target molecule in a precise manner and, therefore, can be integrated into portable laboratory devices on a chip. Our vision entails a practical implementation method that revolves around the detection of pesticides. This can be achieved by analyzing the drain water or conducting individual tests while washing vegetables and fruits.

ASSOCIATED CONTENT

Supporting Information

The Supporting Information is available free of charge at https://pubs.acs.org/doi/10.1021/acs.langmuir.3c00822.

Sensing glyphosate with modified carbon fiber electrodes containing 1 and 5 μM aptamers, details on the LOD calculation procedure, AFM image of the functionalized CF electrode, and open-circuit potential measurements in the presence of PMIDA and AMPA (PDF)

AUTHOR INFORMATION

Corresponding Author

Ekaterina V. Skorb − *ITMO University, Saint Petersburg 191002, Russian Federation;* orcid.org/0000-0003-0888-1693; Email: skorb@itmo.ru

Authors

Ksenia A. Rukhlyada − *ITMO University, Saint Petersburg 191002, Russian Federation*

Victoria V. Matytcina − *ITMO University, Saint Petersburg 191002, Russian Federation*

Anna A. Baldina − *ITMO University, Saint Petersburg 191002, Russian Federation*

Olga Volkova − *ITMO University, Saint Petersburg 191002, Russian Federation;* orcid.org/0000-0002-5812-6162

Dmitry A. Kozodaev − *NT-MDT BV, 7335 Apeldoorn, The Netherlands*

Nadezhda V. Barakova − *ITMO University, Saint Petersburg 191002, Russian Federation*

Olga Yu. Orlova − *ITMO University, Saint Petersburg 191002, Russian Federation*

Evgeny Smirnov − *ITMO University, Saint Petersburg 191002, Russian Federation;* orcid.org/0000-0001-7930-7758

Complete contact information is available at: https://pubs.acs.org/10.1021/acs.langmuir.3c00822

Author Contributions

#K.A.R. and V.V.M. contributed equally.

Notes

The authors declare no competing financial interest.

ACKNOWLEDGMENTS

This work was supported by the following research grants: RSF grant no. 21-13-00403. E.S. acknowledges the ITMO Fellowship Program for the financial support. The authors acknowledge Dr. Alexey Sviridov for the help with aminomethylphosphonic acid (AMPA) and *N*-(phosphonomethyl)iminodiacetic acid (PMIDA).

ABBREVIATIONS

CV-cyclic voltammetry
LbL-layer-by-layer method
PEI-polyethyleneimine
PSS-poly(sodium 4-styrenesulfonate)
QCM-quartz crystal microbalance
PBS-phosphate-buffered saline
CF-carbon fiber
MCF-modified carbon fiber
SPC-screen-printed electrode

REFERENCES

(1) Duke, S. O. The History and Current Status of Glyphosate. *Pest Manage. Sci.* **2018**, *74*, 1027−1034.

(2) Rani, M.; Shanker, U. Degradation of Traditional and New Emerging Pesticides in Water by Nanomaterials: Recent Trends and Future Recommendations. *Int. J. Environ. Sci. Technol.* **2018**, *15*, 1347−1380.

(3) Belfroid, A. C.; van Drunen, M.; Beek, M. A.; Schrap, S. M.; van Gestel, C. A. M.; van Hattum, B. Relative Risks of Transformation Products of Pesticides for Aquatic Ecosystems. *Sci. Total Environ.* **1998**, *222*, 167−183.

(4) Aga, D. S.; Thurman, E. M. Formation and Transport of the Sulfonic Acid Metabolites of Alachlor and Metolachlor in Soil. *Environ. Sci. Technol.* **2001**, *35*, 2455−2460.

(5) Zahm, S. H.; Ward, M. H. Pesticides and Childhood Cancer. *Environ. Health Perspect.* **1998**, *106*, 893−908.

(6) Swanson, N. L.; Leu, A.; Abrahamson, J.; Wallet, B. Genetically engineered crops, glyphosate and the deterioration of health in the United States of America. *J. Org. Syst.* **2014**, *9*, 6−37. https://www.organic-systems.org/journal/92/abstracts/Swanson-et-al.html

(7) Goel, A.; Aggarwal, P. Pesticide poisoning. *Natl. Med. J. India* **2007**, *20*, 182−191. https://pubmed.ncbi.nlm.nih.gov/18085124/

(8) Bassil, K. L.; Vakil, C.; Sanborn, M.; Cole, D. C.; Kaur, J. S.; Kerr, K. J. Cancer health effects of pesticides: systematic review. *Can. Fam. Physician* **2007**, *53*, 1704−1711. https://pubmed.ncbi.nlm.nih.gov/17934034/

(9) Gunarathna, S.; Gunawardana, B.; Jayaweera, M.; Manatunge, J.; Zoysa, K. Glyphosate and AMPA of Agricultural Soil, Surface Water, Groundwater and Sediments in Areas Prevalent with Chronic Kidney Disease of Unknown Etiology, Sri Lanka. *J. Environ. Health, Part B* **2018**, *53*, 729−737.

(10) Van Bruggen, A. H. C.; He, M. M.; Shin, K.; Mai, V.; Jeong, K. C.; Finckh, M. R.; Morris, J. G., Jr. Environmental and Health Effects of the Herbicide Glyphosate. *Sci. Total Environ.* **2018**, *616-617*, 255−268.
(11) Valle, A. L.; Mello, F. C. C.; Alves-Balvedi, R. P.; Rodrigues, L. P.; Goulart, L. R. Glyphosate Detection: Methods, Needs and Challenges. *Environ. Chem. Lett.* **2019**, *17*, 291−317.
(12) Gauglitz, G.; Wimmer, B.; Melzer, T.; Huhn, C. Glyphosate Analysis Using Sensors and Electromigration Separation Techniques as Alternatives to Gas or Liquid Chromatography. *Anal. Bioanal. Chem.* **2018**, *410*, 725−746.
(13) Hernández, F.; Pozo, Ó. J.; Sancho, J. V.; López, F. J.; Marín, J. M.; Ibáñez, M. Strategies for Quantification and Confirmation of Multi-Class Polar Pesticides and Transformation Products in Water by LC−MS2 Using Triple Quadrupole and Hybrid Quadrupole Time-of-Flight Analyzers. *TrAC, Trends Anal. Chem.* **2005**, *24*, 596−612.
(14) Hooijschuur, E. W. J.; Kientz, C. E.; Dijksman, J.; Brinkman, U. A. T. Potential of Microcolumn Liquid Chromatography and Capillary Electrophoresis with Flame Photometric Detection for Determination of Polar Phosphorus-Containing Pesticides. *Chromatographia* **2001**, *54*, 295−301.
(15) Picó, Y.; Blasco, C.; Font, G. Environmental and Food Applications of LC-Tandem Mass Spectrometry in Pesticide-Residue Analysis: An Overview. *Mass Spectrom. Rev.* **2004**, *23*, 45−85.
(16) Oppliger, S. R.; Münger, L. H.; Nyström, L. Rapid and Highly Accurate Detection of Steryl Glycosides by Ultraperformance Liquid Chromatography−Quadrupole Time-of-Flight Mass Spectrometry (UPLC-Q-TOF-MS). *J. Agric. Food Chem.* **2014**, *62*, 9410−9419.
(17) Roda, A.; Michelini, E.; Zangheri, M.; Di Fusco, M.; Calabria, D.; Simoni, P. Smartphone-Based Biosensors: A Critical Review and Perspectives. *TrAC, Trends Anal. Chem.* **2016**, *79*, 317−325.
(18) Mehrotra, P. Biosensors and Their Applications − A Review. *J. Oral. Biol. Craniofac. Res.* **2016**, *6*, 153−159.
(19) Liu, M.; Khan, A.; Wang, Z.; Liu, Y.; Yang, G.; Deng, Y.; He, N. Aptasensors for Pesticide Detection. *Biosens.* **2019**, *130*, 174−184.
(20) Majdinasab, M.; Daneshi, M.; Louis Marty, J. Recent Developments in Non-Enzymatic (Bio)Sensors for Detection of Pesticide Residues: Focusing on Antibody Aptamer and Molecularly Imprinted Polymer. *Talanta* **2021**, *232*, No. 122397.
(21) Wang, J. DNA Biosensors Based on Peptide Nucleic Acid (PNA) Recognition Layers. A review1This Paper Was a Finalist for the Biosensors & Bioelectronics Award for the Most Original Contribution to the Congress.1. *Biosens* **1998**, *13*, 757−762.
(22) Song, S.; Wang, L.; Li, J.; Fan, C.; Zhao, J. Aptamer-Based Biosensors. TrAC. *TrAC, Trends Anal. Chem.* **2008**, *27*, 108−117.
(23) Xie, M.; Zhao, F.; Zhang, Y.; Xiong, Y.; Han, S. Recent Advances in Aptamer-Based Optical and Electrochemical Biosensors for Detection of Pesticides and Veterinary Drugs. *Food Control* **2022**, *131*, No. 108399.
(24) Liu, Y.; Deng, Y.; Li, T.; Chen, Z.; Chen, H.; Li, S.; Liu, H. Aptamer-Based Electrochemical Biosensor for Mercury Ions Detection Using AuNPs-Modified Glass Carbon Electrode. *J. Biomed. Nanotechnol.* **2018**, *14*, 2156−2161.
(25) Alshaer, W. *Functionalizing liposomes with aptamers for active targeting of tumor cells*. https://theses.hal.science/tel-01500095.
(26) Terse-Thakoor, T.; Punjiya, M.; Matharu, Z.; Lyu, B.; Ahmad, M.; Giles, G. E.; Owyeung, R.; Alaimo, F.; Shojaei Baghini, M.; Brunyé, T. T.; Sonkusale, S. Thread-Based Multiplexed Sensor Patch for Real-Time Sweat Monitoring. npj Flex. *Electron.* **2020**, *4*, 18.
(27) Hyder, M.; Shah, N. J.; Hammond, P. T. Design and Translation of Nanolayer Assembly Processes: Electrochemical Energy to Programmable Pharmacies. *Multilayer Thin Films* **2012**, 393−435.
(28) Liu, N.; Jiang, Y.; Zhou, Y.; Xia, F.; Guo, W.; Jiang, L. Two-Way Nanopore Sensing of Sequence-Specific Oligonucleotides and Small-Molecule Targets in Complex Matrices Using Integrated DNA Supersandwich Structures. *Angew. Chem., Int. Ed.* **2013**, *52*, 2007−2011.
(29) Skorb, E. V.; Shchukin, D. G.; Möhwald, H.; Sviridov, D. V. Photocatalytically-Active and Photocontrollable Coatings Based on Titania-Loaded Hybrid Sol−Gel Films. *J. Mater. Chem.* **2009**, *19*, 4931.
(30) Ying, Y.-L.; Yang, J.; Meng, F.-N.; Li, S.; Li, M.-Y.; Long, Y.-T. A Nanopore Phosphorylation Sensor for Single Oligonucleotides and Peptides. *Research* **2019**, *2019*, No. 1050735.
(31) Quinn, J. F.; Yeo, J. C. C.; Caruso, F. Layer-by-Layer Assembly of Nanoblended Thin Films: Poly(Allylamine Hydrochloride) and a Binary Mixture of a Synthetic and Natural Polyelectrolyte. *Macromolecules* **2004**, *37*, 6537−6543.
(32) Josse, F.; Lee, Y.; Martin, S. J.; Cernosek, R. W. Analysis of the Radial Dependence of Mass Sensitivity for Modified-Electrode Quartz Crystal Resonators. *Anal. Chem.* **1998**, *70*, 237−247.
(33) Magna, G.; Belugina, R.; Mandoj, F.; Catini, A.; Legin, A. V.; Paolesse, R.; Di Natale, C. Experimental Determination of the Mass Sensitivity of Quartz Microbalances Coated by an Optical Dye. *Sens. Actuators, B* **2020**, *320*, No. 128373.
(34) Nikolaev, K. G.; Kalmykov, E. V.; Shavronskaya, D. O.; Nikitina, A. A.; Stekolshchikova, A. A.; Kosareva, E. A.; Zenkin, A. A.; Pantiukhin, I. S.; Orlova, O. Y.; Skalny, A. V.; Skorb, E. V. ElectroSens Platform with a Polyelectrolyte-Based Carbon Fiber Sensor for Point-of-Care Analysis of Zn in Blood and Urine. *ACS Omega* **2020**, *5*, 18987−18994.
(35) El-Moghazy, A. Y.; Amaly, N.; Istamboulie, G.; Nitin, N.; Sun, G. A Signal-on Electrochemical Aptasensor Based on Silanized Cellulose Nanofibers for Rapid Point-of-Use Detection of Ochratoxin A. *Microchim. Acta* **2020**, *187*, 1.
(36) Scanlon, M. D.; Peljo, P.; Méndez, M. A.; Smirnov, E.; Girault, H. H. Charging and Discharging at the Nanoscale: Fermi Level Equilibration of Metallic Nanoparticles. *Chem. Sci.* **2015**, *6*, 2705−2720.
(37) Bard, A. J.; Ketelaar, J. A. A. Encyclopedia of Electrochemistry of the Elements. *J. Electrochem. Soc.* **1976**, *123*, 348C−348C.
(38) Pershina, L. V.; Grabeklis, A. R.; Isankina, L. N.; Skorb, E. V.; Nikolaev, K. G. Determination of Sodium and Potassium Ions in Patients with SARS-Cov-2 Disease by Ion-Selective Electrodes Based on Polyelectrolyte Complexes as a Pseudo-Liquid Contact Phase. *RSC Adv.* **2021**, *11*, 36215−36221.
(39) Stekolshchikova, A. A.; Radaev, A. V.; Orlova, O. Y.; Nikolaev, K. G.; Skorb, E. V. Thin and Flexible Ion Sensors Based on Polyelectrolyte Multilayers Assembled onto the Carbon Adhesive Tape. *ACS Omega* **2019**, *4*, 15421−15427.

https://doi.org/10.1021/acs.langmuir.3c00822
Langmuir 2023, 39, 10820−10827